Engineering Geology 283 (2021) 106023

Contents lists available at ScienceDirect

Engineering Geology

journal homepage: www.elsevier.com/locate/enggeo

Analysis of instabilities in the Basque Coast Geopark coastal cliffs for its environmentally friendly management (Basque-Cantabrian basin, northern Spain)

Tomás Morales [a], Jon Ander Clemente [a,*], Laura Damas Mollá [a], Eñaut Izagirre [a,b], Jesus A. Uriarte [a]

[a] Department of Geodynamics, Science and Technology Faculty, University of the Basque Country UPV/EHU, P.O. Box 644, E-48080 Bilbao, Spain
[b] Basque Centre for Climate Change BC_3, Leioa, Spain

ARTICLE INFO

Keywords:
Coastal cliffs
Stability analysis
2D-3D simulation
Friendly management
Basque Coast Geopark

ABSTRACT

Coastal cliffs provide a high landscape value to many natural sites around the world. This means that an ever-increasing number of people are attracted to them. At this point, there is a growing need to manage these spaces from the safety of visitors, but with a view to preserving the environment. With this aim, this paper presents an approach to analyze and manage instabilities in these environments, particularly those subjected to significant anthropic activity, which has been implemented in the cliffs of the Basque Coast Geopark. The starting point is a detailed topographic information, obtained from UAV flights, and the identification on site of unstable elements, including their typology, active source areas, dynamics and reach. From this information, the simulation of rockfall processes, which basically correspond to toppling and infinite slope instabilities favored by differential erosion along the coastline, is approached in two and three dimensions. Results allow the design of precise actions by sectors, according to the energy, height and reach of the detached blocks, including barriers, middle slope actions, ditches and information strategies, depending on the different uses of the sectors. Therefore, this approach leads to a more detailed and environmentally friendly management of these environments.

1. Introduction

Coastal cliffs are geological-geomorphological elements that give rise to unique landscapes of high scientific, cultural and social value on coasts around the world (Emery and Kuhn, 1982; Panizza, 2001; Kubalíková, 2013; Kirchner and Kubalíková, 2013; Kirchner and Kubalíková, 2015; Young, 2018). Defined as a steeply sloping surface where elevated land meets the shoreline (Hampton and Griggs, 2004), constitute about 80% of the world seashore (Emery and Kuhn, 1982). Rising above the geological outcrops developed on a wave-cut platform, upon beaches or directly over the sea (Trenhaile, 2010; Sunamura, 2015) are affected by different marine and subaerial processes (Alessio and Keller, 2020), including waves (Young et al., 2011), groundwater flow (Pierre and Lahousse, 2006), mechanical and chemical weathering (Porter and Trenhaile, 2007) and rainfall (Collins and Sitar, 2007); while acting as conditioning factors the cliff lithology (Sunamura, 1992), coast geometry (Hampton and Griggs, 2004) and structural characteristics (Duperret et al., 2004).

Some of them are recognized and recognizable natural settings that attract an increasingly large audience. A particularly significant example of this situation is the Basque Coast Geopark (Geoparkea).

This protected area extends over 14 km from the eastern coast of the Basque Country (northern Spain). It is dominated by cliffs, with outcrops of high geological value, as evidenced by the award of two golden spikes ratified in 2010 by the International Commission on Stratigraphy (ICS), part of the International Union of Geological Sciences (IUGS). In November 2010, it joined the European and Global Network of Geoparks, which brings together sites of international geological importance, managed with values of conservation, education and sustainable development (Black and Gonggrijp, 1990; Brilha, 2002; Andrasanu, 2009; Henriques et al., 2011; Wimbledon and Smith-Meyer, 2012; Brilha, 2018).

Within this protected environment, the most visited sectors are those corresponding to the beaches of Itzurun and Algorri, together with the cliffs around the village of Zumaia. Given that the Basque coast is predominantly erosive, these beaches attract significant summer tourism. In

* Corresponding author.
E-mail address: jonander.clemente@ehu.eus (J.A. Clemente).

https://doi.org/10.1016/j.enggeo.2021.106023
Received 3 July 2020; Received in revised form 3 December 2020; Accepted 29 January 2021
Available online 1 February 2021

addition, cult films and series have been filmed in the area in recent times, which has led to a significant increase in the number of visitors throughout the year.

It is a natural environment of active dynamics, where coastal cliffs evolve through gravitational processes, with the development of different forms of instability, resulting in rockfalls (Canuti et al., 2009), which is one of the most recurrent processes in coastal environments (Rosser et al., 2005; Michoud et al., 2012).

In this context, the need arises to know in detail the evolutionary processes that condition safety in the area. To this end, it is essential to analyze the factors and conditions of their origin (Luckman, 2013; Hernández-Gutiérrez and Santamarta, 2015), with the aim of carrying out specific risk management (Glade, 2003; Crosta and Agliardi, 2004; Frattini et al., 2008, 2012). However, unlike usual slope engineering projects, conservation and stabilization attempts in environments of recognized natural and cultural value must not only address the damage that may be generated, but also the need to maintain their natural condition when intervening on the site (Guo et al., 2009; Margottini and Vilímek, 2014; Morales et al., 2018).

The work therefore acquires a new complexity (Margottini et al., 2016), since the measures and ways of acting must be effective, to solve the problem; non-invasive, to preserve the original aspect of the site; and feasible with the use of techniques that involve the protection and development of the environment. The nature and purpose of these measures can be completed with the recommendations of the ICOMOS (2003), among which it can be highlighted that each intervention should be proportional to the previously established safety objectives, and limited to the minimum necessary to guarantee the safety and durability of the property, with the least possible damage to the heritage values. An additional recommendation would be that the actions be reversible. The implementation of this approach in the study of instability processes requires a detailed information about the terrain (Abellán et al., 2010; Pham et al., 2016; Fanos and Pradhan, 2019) to develop precise simulation and modeling analyzes (Dorren, 2003; Lan et al., 2007; Stoffel et al., 2010; Keskin, 2013; Ansari et al., 2018), which will allow the proposals for action to be adjusted to the dynamics of the environment under study.

In our work, we seek to make progress in the recognition of instability processes in the Basque Coast Geopark (Geoparkea), which preserves a natural environment including Itzurun and Algorri beaches, with the aim of proposing environmentally friendly management strategies and protection measures in this protected area.

2. Geoparkea study area

The Basque Coast Geopark (Geoparkea) is located in the Bay of Biscay, to the west of the Pyrenees, and covers the villages of Deba, Mutriku and Zumaia (Fig. 1) (https://geoparkea.eus/es/).

Geologically (Fig. 2), this Geopark is located in the so-called Basque-Cantabrian basin (Feuillée and Rat, 1971; Ramírez del Pozo, 1973). There, in a basin-bottom marine environment, thick sedimentary series were deposited during the Lower Cretaceous - Eocene, characterized by a persistent and well-defined stratification, with a great lateral continuity. During the Alpine Orogeny, these materials underwent a notable deformation, giving rise to a mountainous relief that constitutes the western continuation of the Pyrenean mountain range (Arz et al., 1992; Baceta et al., 2012; Barnolas and Pujalte, 2004).

Specifically, the study area corresponds to the coastline between Deba (Sakoneta) and Zumaia, where the geological record is practically continuous from the Maastrichtian (Upper Cretaceous) to the Ypresian (Lower Eocene). The subvertical arrangement of the flyschoid successions allows a precise analysis of them, which concluded with the award of two golden spikes in 2010, a fundamental milestone for the declaration of this space as part of the Global Geoparks Network. Both milestones are located at the Itzurun beach (Zumaia). To the east of it, the boundary between the Danian and the Selandian, associated with a drop in sea level (Orue-Etxebarria et al., 2007; Arenillas et al., 2008; Bernaola et al., 2009), is the first of the two strata marked with the "golden spike". Further to the northeast is the Itzurun Formation, in which the stratotype for the Selandian-Thanetian boundary (golden spike), defined by an inversion in the Earth's magnetic field (Pujalte et al., 1995; Schmitz et al., 1998; Schmitz et al., 2011), has also been awarded.

With respect to the hydrodynamic setting, the study area is exposed to large storms and preferential winds from the NW, which develop waves to SE orientation that dominate all the Basque Coast (Galparsoro et al., 2010; Bilbao-Lasa et al., 2020). These waves rarely exceed 5 m high, and the most habitual height is between 1 and 2 m for summer and 2–5 m for winter. The tidal wave is semi-diurnal and the main tidal range along the Basque Coast is approximately 1.65 m on neap tides and 4.01 m on springs (REDMAR, 2005).

The current landscape is made up of coastal cliffs with heights of between 30 and 70 m that stand out on a coastline dominated by the current wave-cut platforms (Genna et al., 2005; González-Amuchastegui et al., 2005; Pedoja et al., 2014). Coastal dynamics condition that, in areas protected from the action of waves and marine currents, beaches such as the aforementioned Itzurun beach are developed (Bird, 2000;

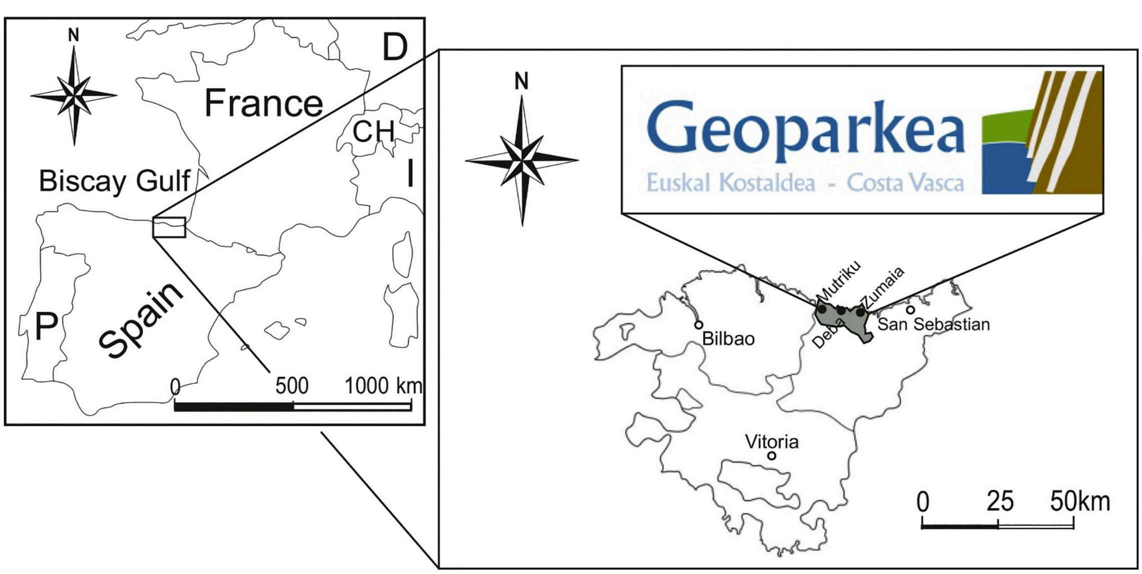

Fig. 1. Geographical context of the Basque Coast Geopark.

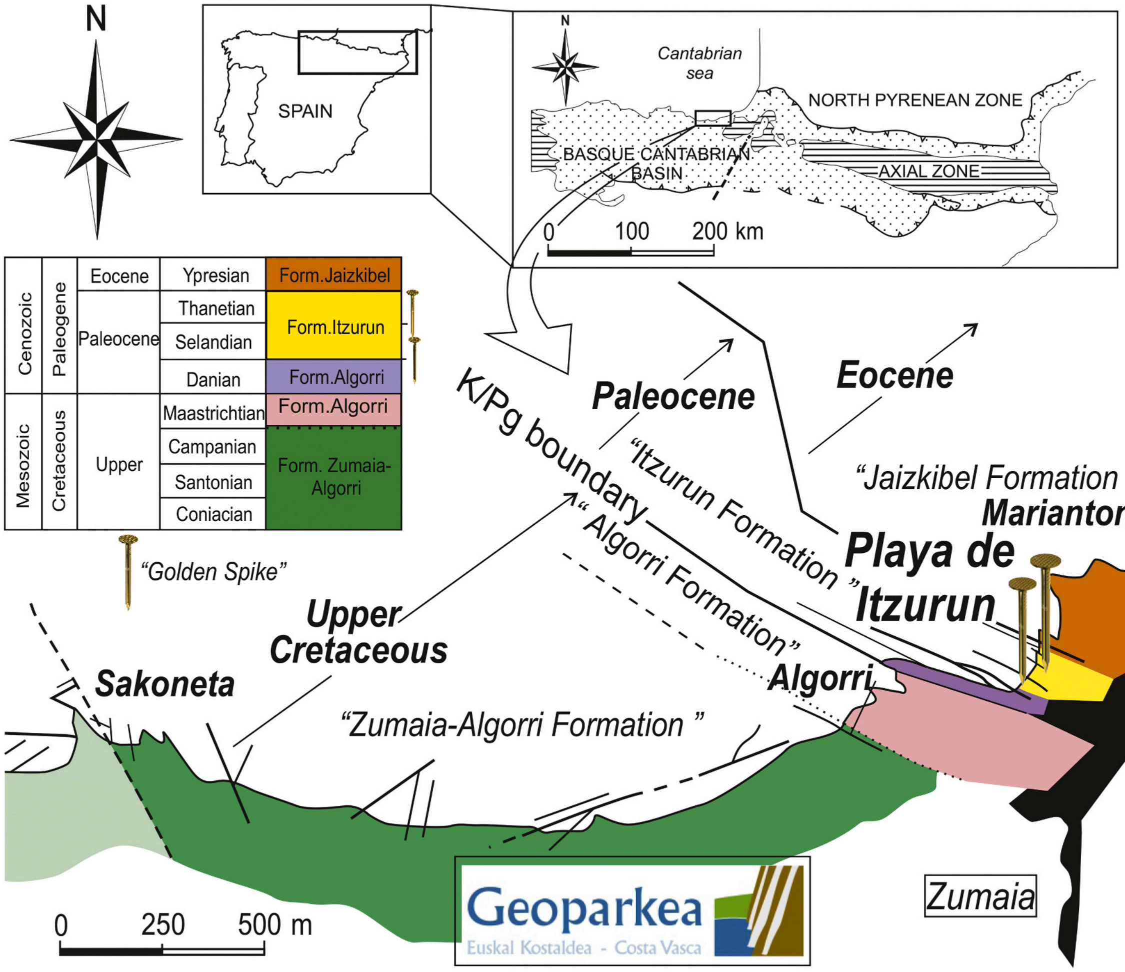

Fig. 2. Sketch map of the main structural features of the Pyrenean belt (modified from Boillot and Capdevila, 1977) and geological map of the studied zone in the Basque Coast Geopark (modified from Baceta et al., 2012).

Álvarez-Marrón et al., 2008; Gutiérrez-Elorza, 2008). These are, however, localized and scarce geomorphological elements, and hence they concentrate notable summer tourism. This combination of landscape, geological and leisure values, has led to a growing influx of general and specialized tourism into the area, which is why the study of stability and safety of the cliffs and their management in a high-value environment is a challenge and a necessity.

3. Methodology

3.1. Detailed topographic information

The first phase of the work consisted of obtaining a detailed image of the terrain, for which we acquired aerial imagery using a commercial DJI Mavic Pro 2 drone or unmanned aerial vehicle (UAV). The UAV is equipped with a 20 Megapixel digital compact camera with a fixed 28-mm lens and we added a Reach M+ RTK (Real Time Kinematic) device that was in continuous radio communication with a base EMLID Reach RS+ station. This technique is widely used for topography, where a single reference station provides corrections to a rover device in real time, obtaining a submetric accuracy (Raquet and Lachapelle, 2001; Wu et al., 2019; Valente et al., 2020).

The UAV was launched from the highest parts of the cliffs at 40 m above launch points, and the survey plan, designed with the assistance of a 1 m resolution LIDAR mosaic, provided a consistent flight altitude of ~80 m above sea level and a ground sampling distance (GSD) of ~3 cm per pixel. Flights were planned with the flight planning software Pix4Dcapture and the UAV flight speed was set to 6 m/s. For all flights, the overlap of both front and side images was set to be 70%, although the real overlap is supposed to be even larger because most of the modelled terrain lies lower than the UAV launching points from the highest part of the cliffs.

Photogrammetric outputs were calculated from images and camera positions using Agisoft Metashape Professional v1.6.3 software (https://www.agisoft.com/). Processing workflow and parameters were set according to official Agisoft guidelines (Agisoft, 2018), and Structure from Motion (SfM) algorithm was used to create the final dense point cloud, from where the orthomosaics at 0.15 m resolution and geoid-corrected Digital Terrain Models (DTMs) at 0.20 m resolution were derived. The SfM technique is highly employed in the field of geosciences (Westoby et al., 2012; Jing et al., 2017; Feurer and Vinatier, 2018), which allows obtaining a high-resolution data, capable of representing a 2D to 3D object with a series of photographs from different points of view (Tomás et al., 2016; Kim et al., 2018; Garrido-Carretero et al., 2019; Zhang et al., 2020) (Fig. 3).

3.2. Identification of unstable elements

Instabilities are identified directly on site, through monthly visits during the last 2 years, which were documented photographically. Survey is completed, particularly in not accessible areas, with the images of the UAV. Fieldwork also includes the characterization of materials and discontinuity network that affect the rock mass. This network gives rise to a structure of planes of weakness that determine the shape

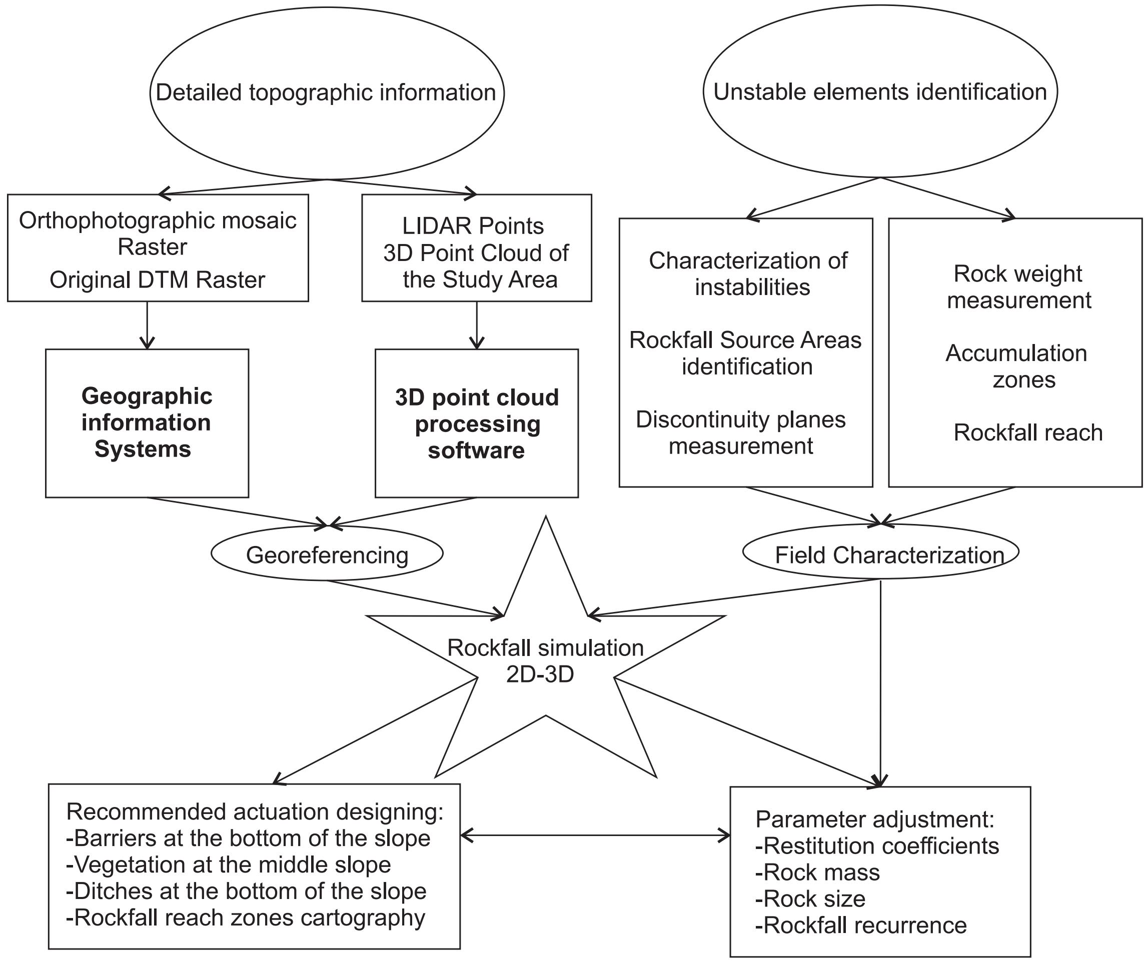

Fig. 3. Methodological flow chart.

and size of the unstable elements. Furthermore, their orientation with respect to the cliffs determines the dynamics of the instabilities. Its characterization includes the measurement of the orientation of the discontinuity planes and their geomechanical characteristics (roughness, filling, opening and spacing) (Fraternali, 2007; Zhang et al., 2018; Kong et al., 2020). Based on these measurements, the different discontinuity families of slope are established, and a kinematic analysis of instabilities in stereographic projection is performed. In our case, RocScience's Dips.v.6.0. software (RocScience, 2013) is used to facilitate data processing. With this information, the types of instabilities, active rockfall source areas, evolution and reach are defined.

At the same time, a specific recognition of the detached blocks was carried out, which includes the collection of data on their weights and morphologies, fall trajectories and reaches. The determination of weights was done with two KAMER model dynamometers: one for rocks up to 25 kg, with an accuracy range of +/− 20 g; the other for rocks up to 150 kg, with an accuracy range of +/− 100 g. The size of the rocks was obtained with a measuring tape that the same dynamometer incorporates. The weight and dimensional measurements were made on the rocks deposited at the foot of the slope, along with the quantification of the number of falls, their reach, the areas of influence and, where observable, the entity of impacts. This section also included information provided by technicians from the Geopark and the City Council.

3.3. Modeling and simulation of rockfalls

The evolution in the terrain of detached rock fragments is controlled by the dissipation of their energy, which is usually approximated by two coefficients (Pfeiffer and Bowen, 1989): the normal restitution coefficient (R_N), which indicated the degree of elasticity in a normal collision with the slope; and the tangential restitution coefficient (R_T), which is a measure of the resistance to the movement parallel to the slope. From both parameters, and after establishing the impact angle, the resulting velocity components can be obtained from the equations (Pfeiffer and Bowen, 1989; Budetta and Santo, 1994; Spadari et al., 2013; Asteriou, 2018; Rebouças et al., 2019; Jiang et al., 2020; Li et al., 2020; Wang et al., 2020):

Reflected normal velocity ($v_{n,\,r}$):

$$v_{n,r=} = \frac{v_{n,i}\cdot Rn}{1+\left(\frac{|v_{n,i}|}{K}\right)^2} \tag{1}$$

where

$v_{n,\,i}$ = incident normal velocity,

K = empirical reference velocity.

Reflected tangential velocity($v_{t,\,r}$)

$$v_{t,r=}\sqrt{\frac{R^2\cdot\left(I\cdot\omega_{(1)}{}^2+m\cdot v_{t,i}{}^2\right)\cdot FF\cdot SF}{I+m\cdot R^2}} \tag{2}$$

where

R = radius of the rock.

$\omega_{(1)}$ = initial rotational velocity.

m = rock mass.

$v_{t,\,i}$= initial tangential velocity.

FF = friction function.

SF =scaling factor.

I = rock moment of inertia.

Considering the final rotational velocity ($\omega_{(2)}$) as:

$$\omega_{(2)} = \frac{v_{t,r}}{R} \quad (3)$$

With a friction function (FF), that considered the energy loose in the collision:

$$FF = \frac{1 - R_T}{1.2 + \left(\frac{v_{t,i} - R\cdot\omega_{(1)}}{k_1}\right)^2} \quad (4)$$

and a scaling factor (SF):

$$SF = \frac{R_T}{1 + \left(\frac{v_{n,i}}{k_2 . Rn}\right)^2} \quad (5)$$

where k_1 and k_2 are empirical reference velocities.

3.3.1. Three-dimensional (3D) rockfall simulation

The rockfall simulation process was approached by using RocPro3D software (RocPro3D, 2014). This software performs three-dimensional simulations of individual trajectories from a Digital Terrain Model (DTM), which is extracted from the three-dimensional point cloud derived from the SfM processing. The same software allows the generation of a three-dimensional terrain mesh by triangulation. The mesh is the basis on which the simulation of rockfall from the identified source areas is carried out. From this simulation, analysis of parameters are mapped onto the DTM, with individual cell sizes over 1 m.

The main advantage of this model, according to the comparative study conducted by Li and Lan (2015), is that it allows the relief to be considered in three dimensions, including the lateral evolution of the trajectories in the simulation. On the contrary, it does not allow modifications to the relief, since it works with the topographic information obtained previously.

3.3.2. Two-dimensional (2D) rockfall simulation

Once the general 3D simulation process is completed, in those cases where fall profile modification is considered, the process is studied locally with RocScience's RocFall software (RocScience, 2004). This software allows performing individualized rockfall simulations (Frattini et al., 2012; Dorren et al., 2013), based on the previously defined 3D fall trajectories. In our approach the main advantage it brings, is that it makes possible to vary the topographic profile (Li and Lan, 2015), and thus, to observe its effect on the evolution of materials. In this 2D simulation process, the topographic profiles previously generated by the RocPro3D software (RocPro3D, 2014) were considered.

3.3.3. Validation of results and proposals for action

The results were ground-truthed with field observations, allowing to check the similarities and differences between the observed data and the simulated ones, and to adjust the calculation parameters of the models.

Once the detailed modeling of each reference area was achieved, and the types of failure, their reach and energy were established, specific actions to minimize the negative effects of rockfalls can be simulated. In our work, we consider a combination of engineered and non-engineered actions, depending on the uses and characteristics of the zone involved. Thus, in the beach access zones, constructed elements (Volkwein et al., 2011), as barriers at the bottom of the slope (Agliardi and Crosta, 2003; Crosta and Agliardi, 2003; Agliardi et al., 2009; Crosta et al., 2015), are complemented with quasi-natural protection measures, as middle slope vegetation (Masuya et al., 2009; Chen et al., 2013) and collection ditches (Lorentz et al., 2010; Lambert and Bourrier, 2013). In zones where the cliff evolves directly to the beach, information campaigns, complemented with panels and flyers are proposed, once the susceptibility map is established.

4. Results

4.1. Characterization of the instabilities in the study area

At Itzurun beach (sector 1, Fig. 4a), the general strata orientation, S_0: 80/010, is mainly perpendicular to the coastline (Fig. 4a, b), with steep dips towards the northeast. The geological materials are arranged in alternating layers of different competition (flysch sequences), with Uniaxial Compressive Strength (UCS) values varying from 30 to 34 MPa for limestone levels to 20–27 MPa for marls and 10–20 MPa for calcareous and sandy siltstones (Morales et al., 2004).

Layers arrangement limits the development of the discontinuity planes that affect the rock mass; in fact, only the stratification (S_0) presents large developments (over 40 m), while the rest of the weakness planes generally present developments of less than a meter. Specifically, these are the families of joints J_1: 70/285, oriented to the beach, and J_2: 20/110, oriented to the inside of the rock mass (Fig. 4a). This orientation of discontinuities is in principle favorable to slope stability and makes the instability processes to be limited, in general, to moderate falls of rock fragments of small dimensions that evolve over J_1 (rock plane failures, Table 1). However, differential erosion results in a succession of headlands and inlets, of different dimensions, which give rise to two types of secondary slopes. One, developed at the top of the most resistant layers, with the same dip as the stratification (obverse), and the other on the opposite side of the overhang (reverse). In the first case, the front of the slope is the resistant stratum, in principle stable, although small layer over layer slides with parallel slope and failure planes (infinite slope type failures, Table 1) may develop. On the reverse side, the resistant materials give rise to an overhanging slope that favors the development of abundant rock fragment topplings (Table 1), which are the main instability processes on the cliffs surrounding Itzurun beach.

To the south of Itzurun beach, differential erosion has given rise to a sharply headland (sector 2, Fig. 4a, c) developed over competent materials. The erosive action of the waves has generated in its front some characteristic arch morphologies that constitute one of the most recognizable images of the Geopark. The general geological structure is favorable to stability; however, in 2019, an infinite slope failure of a stratum plate of 30 cm thickness and several meters of development has been recorded.

Further south of the Itzurun beach, the small beach of Algorri (sector 3, Fig. 4a, d) draws a small inlet flanked by two cliffs that present the typology of failures described for Itzurun. Nevertheless, in a more erosive environment, the development of instabilities is of greater entity. Thus, on the northern slope, where the K-Pg boundary is located, the conditions for the development of topplings are very favorable and the fall of blocks of moderate size is relatively frequent. In the southern slope, developed at the top of a competent layer, an infinite slope failure of similar dimensions to those of sector 2 has been recorded in 2018.

Finally, to the north of the Itzurun beach (sector 4: Itzurun Txiki, Fig. 4e), the flyschoid sequence is similar to sector 1; the main difference with the previous one is that it runs along a wave-cut platform, so the base of the cliffs is of a highly erosive nature. Towards the north, the series become marlier in general and the presence of a smaller number of competent levels is a fundamental factor that determines the development of massive breaks in Punta Mariantón (Fig. 4e), which corresponds to a complex movement (Varnes, 1978).

4.2. Analysis of rockfall at Itzurun beach

4.2.1. Characterization of instabilities

Once the general reconnaissance of the area had been carried out, the work focused on the analysis of falls on the cliffs bordering Itzurun beach (sector 1). This is the most visited area, as well as the one where the accesses to the beach are located.

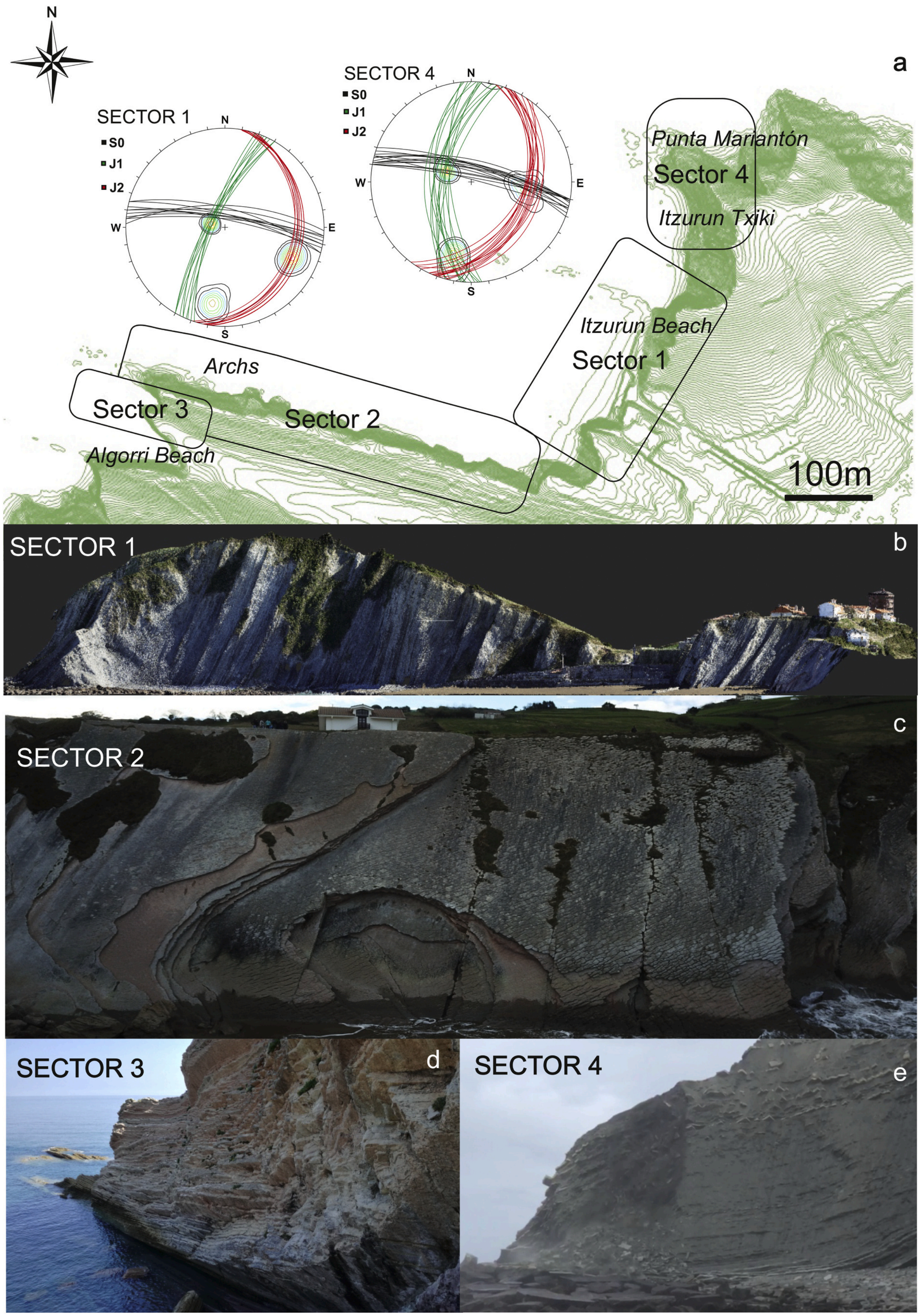

Fig. 4. a) Sectors differentiated in the study area: b) Itzurun beach: corresponds to the area of the most use, where a large part of the summer tourism is concentrated; c) Archs: the beach is framed by spectacularly developed cliffs marked by the presence of large natural arches; d) Algorri beach: where the K/Pg boundary outcrops; e) Punta Mariantón: characterized by coastal cliffs over a wave-cut platform.

Table 1
Typology and main characteristics of instabilities by sectors.

Dip			DipDirection	Type	Recurrence[a]	Size[b]
Sector 1	General slope	80	280	Rock Plane	Moderate	Small
Itzurun beach	Obverse slope	75	030	Infinite Slope	Low	Medium
	Reverse slope	50	200	Toppling	Very high	Medium
Sector 2	General slope	65	020	Infinite Slope	Infrequent	Extraordinary
Archs						
Sector 3	North slope	70	010	Toppling	High	Large
Algorri beach	South slope	75	240	Infinite Slope	Infrequent	Extraordinary
Sector 4	General slope	80	280	Rock Plane	Moderate	Small
Itzurun txiki	Obverse slope	75	030	Infinite Slope	Low	Medium
PuntaMariantón	Reverse slope	50	200	Toppling	Very high	Medium
	South slope	80	190	Massive Slide	Infrequent	Extraordinary

[a] Recurrence: Infrequent: less than 1 per more than 5 years; Very low: less than 10 per 1–5 years; Low: less than 10 per year; Moderate: less than 10 per month; High: less than 10 per week; very high: more than 10 per week.
[b] Size: Small: <1 dm^3; Medium: 1–5 dm^3; Large: 5–25 dm^3; Very large: > 25 dm^3; Extraordinary: several m^3.

There, the origin areas of the rockfalls, or source areas, correspond to the rocky outcrops of the front of the cliffs. The most active areas were identified by fieldwork, determining their height, development, materials involved and landslide marks (Fig. 5a). At the bottom of the slope, the number of accumulated blocks, their location, origin, reach, impact and damage are identified (Fig. 5a).

This fieldwork also allows differentiating the paths followed by the detached blocks. Thus, some blocks fall directly from the front of the cliff to the bottom of the slope, defining an almost straight trajectory. The most frequent rockfalls, however, start with a toppling from the secondary obverse slope and draw a more complex curved evolution to the bottom of the slope.

Altogether, a total of 363 rocks were weighed in the accumulation areas. A lower weight limit of 10 N is taken, which allows collecting the elements of greater energy and reach, avoiding the measure of the smaller elements. From this information, an overall bar diagram was elaborated allowing to observe that most of the fragments have a weight lower than 500 N, and 80% are lower than 100 N. Locally, blocks of more than 5000 N were identified, which represent less than 0.01% of the total (Fig. 5b). The smaller and consequently lighter fragments come mainly from the siltstone layers of the series, while the larger materials come from the more competent ones, which are limestones and marls.

In regards to the reach of the detached fragments, most of the falls are of limited dimensions and the blocks remain accumulated at the foot of the slope. However, some fragments evolve to the access area and to the beach. Their reach, measured from the baseline of the slope, does not exceed 10 m. They are precisely the problems associated with these falls that make it necessary to analyze in detail their dynamics, reach and energy, with a view to designing friendly interventions that prevent damage without substantially disturbing the environment.

4.2.2. Modeling

For the detailed analysis of the detached blocks, the sector of Itzurun beach has been divided into 8 zones (Fig. 5). In each of these, the evolution of materials is simulated on the DTM obtained previously. In the areas with a high number of fallen blocks, a statistical analysis of their weight was carried out and the characteristic parameters of their distribution were obtained. As an example, in areas F and G, the blocks coming from the most competent levels aforementioned, which present greater size, energy and reach (Fig. 6), are adjusted to a normal distribution, considering a lower limit of weight of 100 N. From this, the mean and a superior characteristic value that includes the 95% of sample weights were calculated (Bond and Harris, 2008). Specifically, in the examples of Fig. 6, for a number of samples $n = 54$ and 70, the corresponding characteristic weight values ($t_{n-1}^{95\%}$) are 824 N and 578 N, respectively. In the areas with a smaller number of blocks, the simulations have been carried out with the maximum-recorded sizes.

As for the characteristic parameters of the materials in the slope, they are calibrated to reproduce the trajectories and reach of rock fragments recognized in the fieldwork. In this approach, 4 types of terrains with clearly differentiate mechanical response have been considered in the modeling: flysch, beach, vegetation and access. Flysch is used for the alternating layers of the series that constitute the rocky outcrops; beach corresponds to the sandy zone, with high damping capacity; vegetation is defined as the zone where the rocky outcrops are covered by different types of flora that condition the development of the instability process; finally, access represents pathways constructed with rigid elements.

The characteristic coefficients of restitution, rebound and friction obtained from the adjustment process are shown in Table 2.

From these values, possible random deviations are considered, following Gaussian distributions with the standard deviation values predefined in the RocPro3D software (RocPro3D, 2014) (Table 2).

With the above-mentioned parameters of rock weight, source area and zero initial speed, on the one hand, and those of the four terrains, on the other hand, we launched 100 rockfall simulations per active source area, obtaining a wide representation of trajectories.

For the whole sector, the maximum energy values were obtained in zone G (Table 3, Figs. 5, 6 and 7), where 12 kJ were computed. In the rest of the zones, except for zones A and F, where values of up to 5 kJ were achieved, the maximum values were around 2 kJ (Table 3). The maximum reaches were obtained in zones A and G, with values up to 10 m from the baseline of the slope (Fig. 7). In zones E and F, the current presence of barriers limit the reach of rockfalls.

4.3. Mitigation measures

Unlike usual slope engineering projects, conservation and stabilization efforts in environments of high landscape and environmental value must not only deal with the damage that may be generated, but also with the need to observe the principle of maintaining their natural condition when intervening on the site (Guo et al., 2009).

In accordance with these criteria, the following main mitigation measures are considered in the Basque Coast Geopark:

- Removing loose materials on the cliffs and slopes around the Itzurun beach, with the elimination of unstable elements.
- Protection of the access area by means of barriers in the base or the middle of the slope. The installation of semi-rigid barriers similar to those already existing in zones E and F (Fig. 6) is considered the most recommendable option. These are barriers built with wooden elements of 100 mm diameter, internally reinforced with corrugated steel bars of 10 mm diameter, which have proved to be efficient for blocks of up to 800 N, with impact energies of up to 5 kJ. In each specific zone, barriers of different heights were tested to analyze their capacity of fall interception with the 3D model (Fig. 8a). In those stretches where high barriers (> 2 m) would be required, retention elements at different levels of the slope (middle slope actions) were considered to limit rebounds (Fig. 8b). These actions may

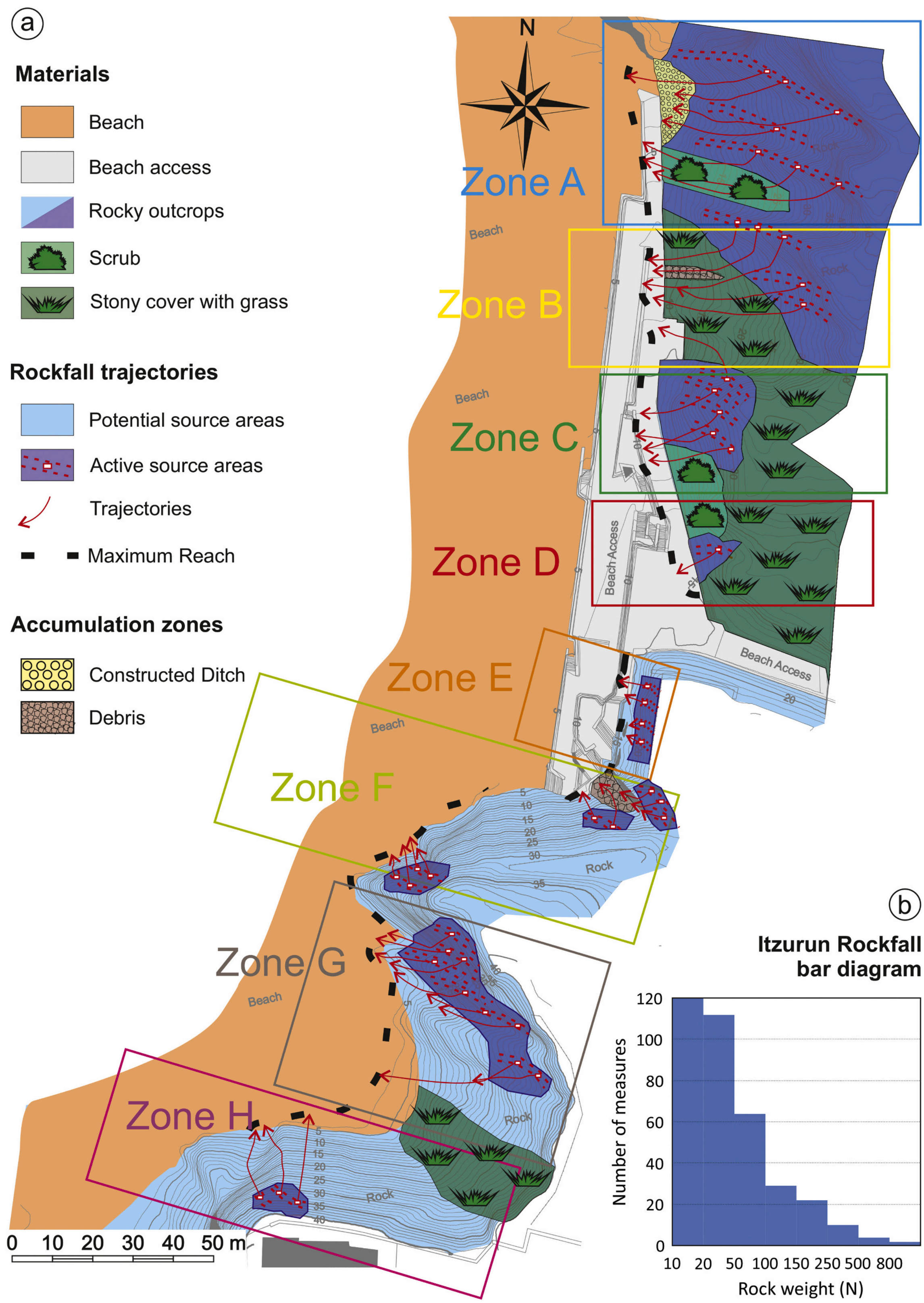

Fig. 5. Rockfall basic information: a) source areas, trajectories and reach of rockfalls at the Itzurun beach; b) bar diagram by weight of fell rocks.

correspond to barriers similar to those previously described or local plantations of shrubs that may favor rock retention in a natural way. Finally, in stretches where the terrain profile allows it, the barriers were complemented with catch areas or benches at the base of the slope. The effectiveness of these last measures cannot be verified with the 3D model, since it does not allow modifications of the relief, so in this case 2D profiles extracted from the three-dimensional trajectories were considered (Fig. 8c).

- Informative and preventive measures at the beach area, beyond the general removing of loose materials on the cliffs. In this sense, local

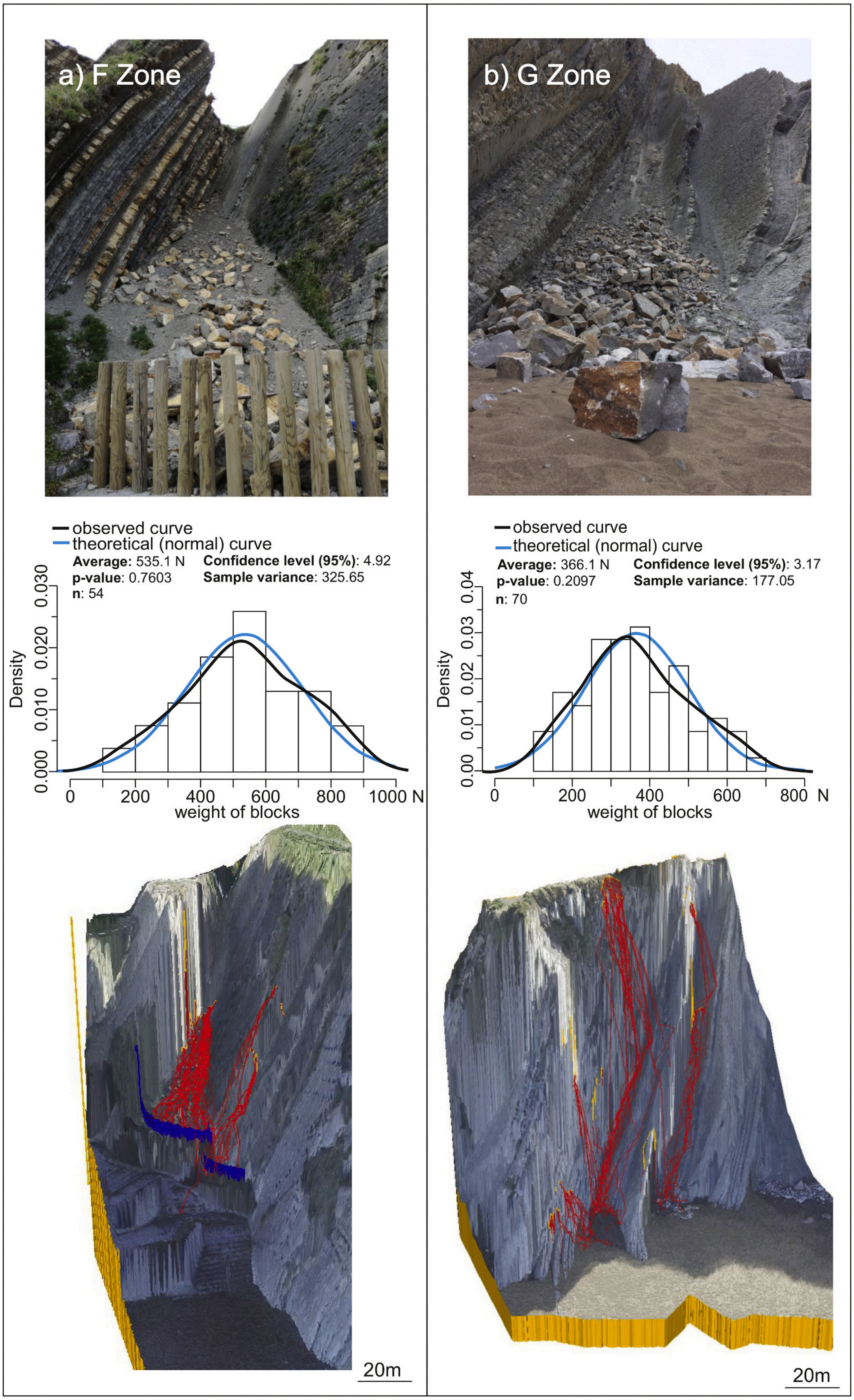

Fig. 6. Photographs, normality analysis and three-dimensional simulations of the F (a) and G (b) zones. On the bottom, 3D models are shown with, the yellow lines corresponding to cliff main active source areas; red lines for simulated individual rockfall trajectories; and blue lines depicting modeled 1-m high barriers. (For interpretation of the references to colour in this figure legend, the reader is referred to the web version of this article.)

Table 2
Terrain adjusted parameters and random deviations considering Gaussian distributions.

Factor	Material	Type	Parameter	Adjusted Value	Prob. Gaussian (μ,σ)
Terrain properties	Flysch	Sliding/Rolling	Dynamic friction (k)	0.45	0.45, 0.045
		Impact	Normal Coefficient of restitution (Rn)	0.6	0.6, 0.011
			Tangential Coefficient of Restitution (Rt)	0.9	0.9, 0.011
			Lateral deviation (°)	0	0, 10
			Rebounds flattening (°)	0	0, 1
	Beach	Sliding/Rolling	Dynamic friction (k)	0.5	0.5, 0.036
		Impact	Normal Coefficient of restitution (Rn)	0.3	0.3, 0.012
			Tangential Coefficient of Restitution (Rt)	0.8	0.8, 0.012
			Lateral deviation (°)	0	0,5
			Rebounds flattening (°)	0	0, 1
	Access	Sliding/Rolling	Dynamic friction (k)	0.6	0.6, 0.036
		Impact	Normal Coefficient of restitution (Rn)	0.6	0.6, 0.0125
			Tangential Coefficient of Restitution (Rt)	0.8	0.8, 0.0125
			Lateral deviation (°)	0	0, 8.75
			Rebounds flattening (°)	0	0, 1
	Vegetation	Sliding/Rolling	Dynamic friction (k)	0.45	0.45, 0.045
		Impact	Normal Coefficient of restitution (Rn)	0.3	0.3, 0.012
			Tangential Coefficient of Restitution (Rt)	0.8	0.6, 0.0125
			Lateral deviation (°)	0	0, 5
			Rebounds flattening (°)	0	0, 1

Table 3
Energy and reach of rockfalls by zones. In zones E and F the reach is limited for barriers.

Itzurun	Zone A	Zone B	Zone C	Zone D	Zone E	Zone F	Zone g	Zone H
Energy (kJ)	3–4	1.5–2.5	0.8–1	0.2	0.2	4–5	12	0.5
Reach (m)	8–10	3–5	3–5	1–2	Barrier	Barrier	8–10	3–5

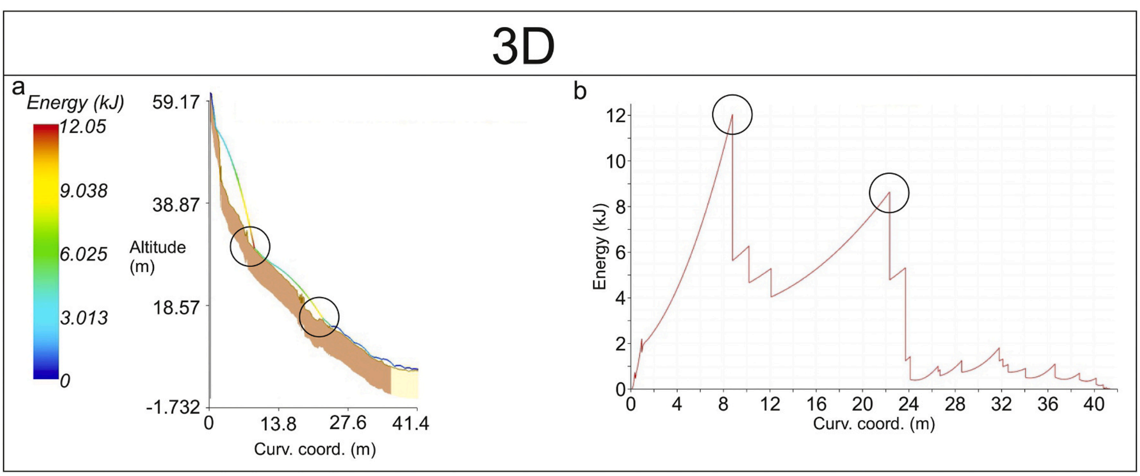

Fig. 7. Individualized analysis of trajectories in the G zone of the Itzurun beach.

population is against taking engineered measures, a condition that is shared by the managers.

Modeling allows the delimitation of rockfall reach with their energy, enabling to establish the corresponding use recommendations. In our case, we define a maximum reach area strip, surrounded by a 2 m preventive zone (Fig. 9). The 2 m preventive zone width corresponds to the grid cell size used in the analysis maps. This information is communicated to users by means of information panels, flyers, digital applications, warning signs and through maintenance personnel.

5. Discussion

The approaches for studying rockfall events are included in three main categories (Shirzadi et al., 2012): empirical models based on relationships between topography and rockfall reach; GIS-based models handling large amounts of geospatial information linked to the development of rockfalls (Evans and Hungr, 1993; Guzzetti et al., 1999; Kaur et al., 2018; Reichenbach et al., 2018; Depountis et al., 2020); and process-based models describing the motion of falling rocks (Pfeiffer and Bowen, 1989; Kobayashi et al., 1990).

Our work deals with the characterization and management of rockfalls in coastal cliffs, where the source areas correspond to the rocky outcrops of the front of the cliffs. The delimited spatial reach of the processes, in a well-defined geomorphological element, facilitates both obtaining direct field measures and simulations using high-resolution digital terrain models. This leads us to use a process-based approach to determine the maximum reach and energy of the detached rock blocks. Direct information promotes an accurate recognition of the susceptibility of the environment from which to establish appropriate control and management measures.

Thus, 2-year field records completed with historical information

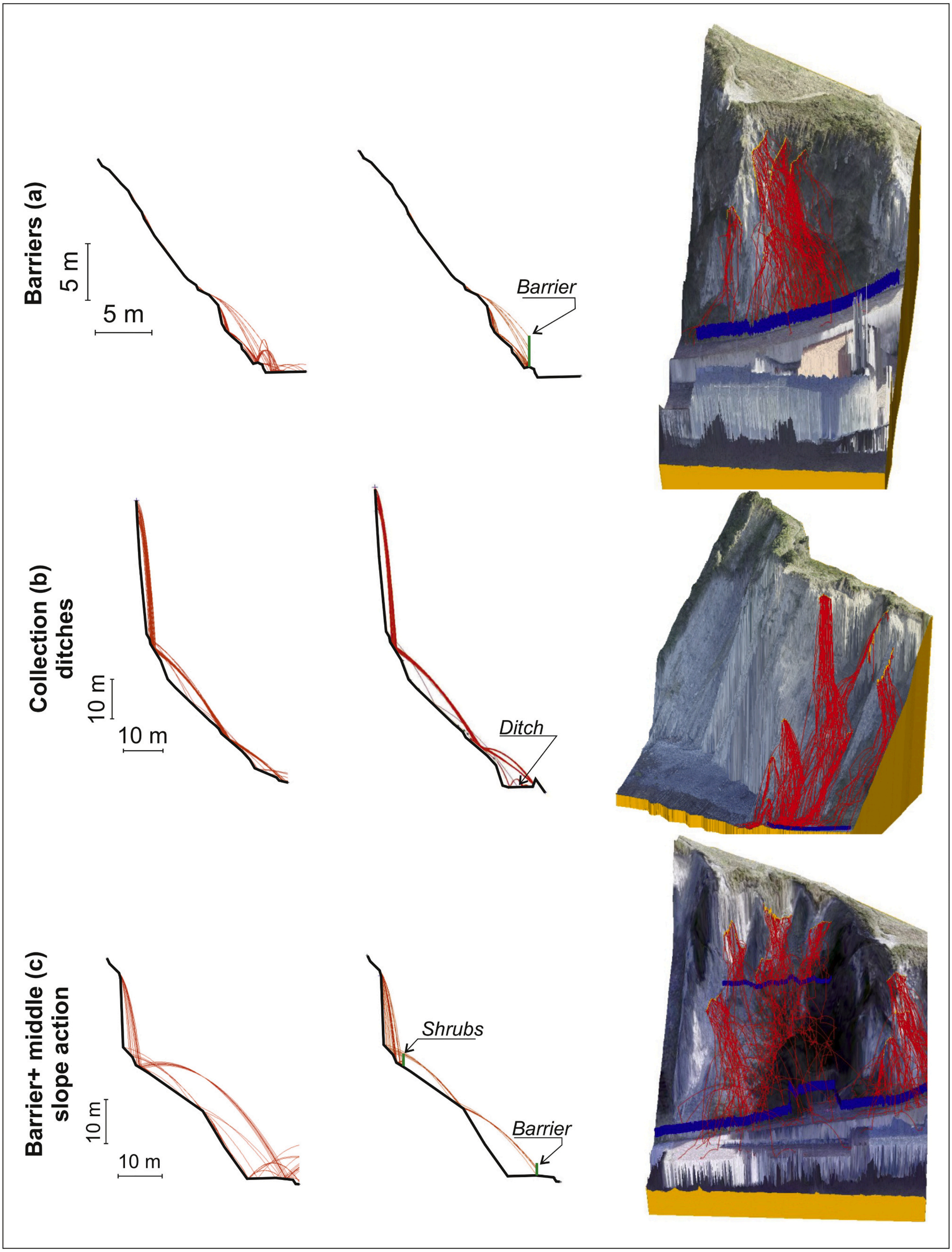

Fig. 8. Current status (left figures) and proposed mitigation actions in 2D (middle figures) and 3D (right figures). a) Rigid barrier; b) collection ditch; c) barrier and actions in the middle slope. The 3D models are shown with, the yellow lines corresponding to cliff main active source areas; red lines for simulated individual rockfall trajectories; and blue lines depicting modeled 1–2 m high barriers. (For interpretation of the references to colour in this figure legend, the reader is referred to the web version of this article.)

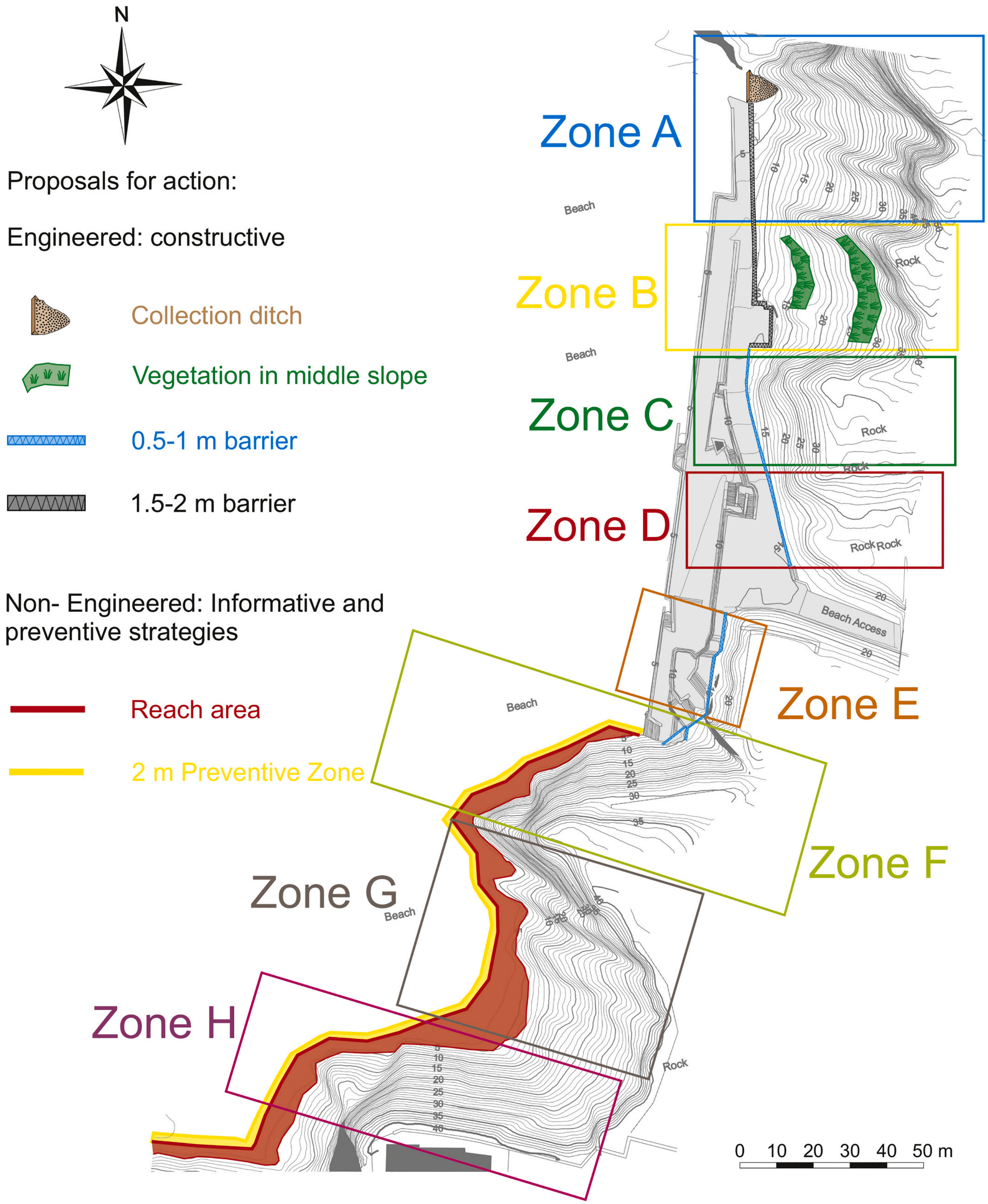

Fig. 9. Map of the recommended measures at the Itzurun beach.

allowed to approach the typology, frequency and entity of the rockfall events in a similar way to rockfall inventories considered in previous works (Bunce et al., 1997; Hungr et al., 1999; Volkwein et al., 2011). At the Itzurun beach, results show (Fig. 5) that the general frequency distribution of rockfall volumes follows a classical power law (Dussauge-Peisser et al., 2003; Hungr et al., 1999; Volkwein et al., 2011). By zones, however, the distribution corresponding to the major blocks (up to 100 N) deposited at the base of the slopes fits a normal density function (Fig. 6). These blocks are originated in the most competent layers of limestones and marls where joint families generate a relatively symmetrical distribution. Rockfall typologies correspond mainly to topplings, with a minor representation of rock plane and infinite slope instabilities.

Rockfall modeling is approached by 3D models. 3D numerical modeling allows including geometrical and dynamic effects of the 3D topography and taking into account the lateral dispersion generating 3D trajectories, overcoming the limitations of 2D models (Volkwein et al., 2011). In our work, a detailed digital terrain model obtained by UAV with a precision of 20 cm is included in RocPro3D software (RocPro3D, 2014). In any case, when changes in the topography are considered the 2D Rocfall software is used (RocScience, 2004).

The first main objective of the modeling effort is to establish the maximum reach and energy of falling blocks. With this aim, the block size considered for design in each differentiated zone corresponds to the 95% of the blocks distribution (as superior characteristic value, Bond and Harris, 2008), where information enough allows a statistical approach, or maximum-recorded sizes if not. Referring to the materials in the slope, 4 types of terrains with clearly differentiate mechanical response were considered. Results were ground-truthed with field observations. In any case, this item presents field of improvement, since the characteristic parameters of materials were obtained through adjustment, and additional experimental determinations and a more detailed characterization of the materials (i.e. based on rock mass classification in the case of rocky outcrops, Hoek, 1994; Morales et al., 2004) will enable us to verify and refine the results.

Once the susceptibility analysis is achieved, management and protection measures are proposed according with the reach and impact energies. In this sense, the information on boulder velocity, jump heights and spatial distribution is the basis for correct design and verification of protective measures (Volkwein et al., 2011). The main limitation in the design of these actions is the development of measures that are harmonious with the environment, avoiding the negative public perception that engineered works may bring (Touili et al., 2014; Ewalt Gray et al., 2017). For the Itzurun beach, as the maximum energy values computed where relative low, up to 12 kJ, protection measures in the access zones include 1–2 m barriers, if necessary combined with middle slope natural buffers, as rows of shrubs, and ditches. The effectiveness of those actions can be approached from guides for standardized barriers (i.e. Volkwein et al., 2019 for flexible systems). In any case, it is more appropriate to maintain unique protective elements, such as existing wooden barriers, whose effectiveness was verified after two events that took place in May and August 2020, adjusting the predicted in this work (Fig. 6a). For the beach sandy zones, at the request of population and managers, not engineered management actions were proposed, but information and warnings of susceptibility.

6. Conclusions

The management of cliffs that all along worldwide coasts join a high landscape and cultural value with a growing attraction of visitors requires the development of specific characterization strategies to assess their susceptibility to instabilities and implement friendly and minimally invasive management strategies to ensure safety.

In this context, this paper deals with the problematic associated with rockfalls in environments where the source areas correspond to the rocky outcrops of the front of the cliffs. In these cases, detailed both topographic information and direct field characterization of rockfall processes allow the development of detailed 3D models, from which to establish susceptibility analysis defining the maximum reach and energy of the detached blocks.

From this information, friendly management strategies may be proposed, having the following priority objectives: to be effective, to solve the problem; minimally invasive, to preserve the natural character of the environment; proportional, in accordance with the established safety objectives; and reversible, to guarantee the durability of the environment.

This comprehensive approach has been proved in the Basque Coast Geopark and can be useful in different spatially well-defined geomorphological environments, not necessarily coastal, with similar processes of instability, particularly in cliff areas enclosing widely visited environments.

Declaration of Competing Interest

None.

Acknowledgements

This study has been carried out by the UPV/EHU Research GroupIT-1029/16 (Government of the Basque Country) in the framework of the strategic project "Analysis of instabilities in coastal environments of the Basque Country" PES-18/97 (University of the Basque Country) and the collaboration of the Basque Coast Geopark (Geoparkea). Finally, the authors are grateful to the reviewers and the handling editor, for the valuable comments that highly improved the paper.

References

Abellán, A., Calvet, J., Vilaplana, J.M., Blanchard, J., 2010. Detection and spatial prediction of rockfalls by means of terrestrial laser scanner monitoring. Geomorphology 119, 162–171. https://doi.org/10.1016/j.geomorph.2010.03.016.

Agisoft, 2018. Agisoft Metashape User Manual: Professional Edition, version 1.5. Agisoft LLC. https://www.agisoft.com/.

Agliardi, F., Crosta, G.B., 2003. High resolution three-dimensional numerical modelling of rockfalls. Int. J. Rock Mech. Min. Sci. 40, 455–471. https://doi.org/10.1016/S1365-1609(03)00021-2.

Agliardi, F., Crosta, G.B., Frattini, P., 2009. Integrating rockfall risk assessment and countermeasure design by 3D modelling techniques. Nat. Hazards Earth Syst. Sci. 9, 1059–1073. https://doi.org/10.5194/nhess-9-1059-2009.

Alessio, P., Keller, E.A., 2020. Short-term patterns and processes of coastal Cliff erosion in Santa Barbara, California. Geomorphology 353, 106994. https://doi.org/10.1016/j.geomorph.2019.106994.

Álvarez-Marrón, J., Hetzel, R., Niedermann, S., Menéndez, R., Marquínez, J., 2008. Origin, structure and exposure history of a wave-cut platform more than 1 Ma in age at the coast of northern Spain: A multiple cosmogenic nuclide approach. Geomorphology 93, 316–334. https://doi.org/10.1016/j.geomorph.2007.03.005.

Andrasanu, A., 2009. Geoeducation, geoparks and geoconservation. In: Proc. 8th European Geoparks Conference: New Challenges with Geoturism. Idanha-a-Nova, Portugal, p. 187.

Ansari, M.K., Ahmad, M., Singh, R., Singh, T.N., 2018. 2D and 3D rockfall hazard analysis and protection measures for Saptashrungi Gad Temple, Vani, Nashik, Maharashtra – A case study. J. Geol. Soc. India 91, 47–56. https://doi.org/10.1007/s12594-018-0819-8.

Arenillas, I., Molina, E., Ortiz, S., Schmitz, B., 2008. Foraminiferal and d13C isotopic event-stratigraphy across the Danian–Selandian transition at Zumaya (northern Spain): chronostratigraphic implications. Terra Nova 20, 38–44. https://doi.org/10.1111/j.1365-3121.2007.00784.x.

Arz, J.A., Canudo, J.I., Molina, E., 1992. Estudio comparativo del Maastrichtiense de Zumaya (Pirineos) y Agost (Béticas) basado en el análisis cuantitativo de los foraminíferos plantónicos. In: Actas III Congreso Geológico de España y VIII Congreso Latinoamericano de Geología, Salamanca, España. Tomo 1, 487–491.

Asteriou, P., 2018. Effect of impact angle and rotational motion of spherical blocks on the coefficients of restitution for rockfalls. Geotech. Geol. Eng. 37, 2523–2533. https://doi.org/10.1007/s10706-018-00774-0.

Baceta, J.I., Orue-Etxebarria, X., Apellaniz, E., Martin-Rubio, M., Bernaola, G., 2012. El Flysch del litoral Deba-Zumaia: una "ventana" a los secretos de nuestro pasado geológico. Servicio Editorial de la Universidad del País Vasco, Bilbao.

Barnolas, A., Pujalte, V. (Eds.), 2004. La Cordillera Pirenaica. In: Vera, J.A. (Ed.), Geología de España. SGE-IGME, Madrid, pp. 233–343.

Bernaola, G., Martín-Rubio, M., Baceta, J.I., 2009. New high resolution calcareous nannofossil analysis across the Danian/Selandian transition at the Zumaia section:

comparison with South Tethys and Danish sections. Geol. Acta 7, 79–92. https://doi.org/10.1344/105.000000272.
Bilbao-Lasa, P., Jara-Muñoz, J., Pedoja, K., Álvarez, I., Aranburu, A., Iriarte, E., Galparsoro, I., 2020. Submerged Marine Terraces Identification and an Approach for Numerical Modeling the Sequence Formation in the Bay of Biscay (Northeastern Iberian Peninsula). Front. Earth Sci. 8, 47. https://doi.org/10.3389/feart.2020.00047.
Bird, E., 2000. Coastal Geomorphology: An Introduction. John Wiley & Sons, New York.
Black, G.P., Gonggrijp, G.P., 1990. Fundamental thoughts on Earth-Science conservation. Jb. Geol. B.-A. 133, 655–657.
Boillot, G., Capdevila, R., 1977. The Pyrenees: Subduction and collision. Earth Planet. Sci. Lett. 35, 151–160. https://doi.org/10.1016/0012-821X(77)90038-3.
Bond, A., Harris, A., 2008. Decoding Eurocode 7. Taylor and Francis, London, pp. 263–304.
Brilha, J., 2002. Geoconservation and protected areas. Environ. Conserv. 29, 273–276. https://doi.org/10.1017/S0376892902000188.
Brilha, J., 2018. Geoheritage and Geoparks. In: Reynard, E., Brilha, J. (Eds.), Geoheritage: Assessment, Protection, and Management. Elsevier, Amsterdam, The Netherlands, pp. 323–335. https://doi.org/10.1016/B978-0-12-809531-7.00018-6.
Budetta, P., Santo, S., 1994. Morphostructural evolution and related kinematics of rockfalls in Campania (southern Italy): A case study. Eng. Geol. 36, 197–210. https://doi.org/10.1016/0013-7952(94)90004-3.
Bunce, C.M., Cruden, D.M., Morgenstern, N.R., 1997. Assessment of the hazard from rock fall on a highway. Can. Geotech. J. 34, 344–356. https://doi.org/10.1139/cgj-34-3-344.
Canuti, P., Margottini, C., Fanti, R., Bromhead, E.N., 2009. Cultural heritage and landslides: Research for risk prevention and conservation. In: Sassa, K., Canuti, P. (Eds.), Landslides – Disaster risk reduction. Springer, Berlin, Heidelberg, pp. 401–433. https://doi.org/10.1007/978-3-540-69970-5_22.
Chen, G., Zheng, L., Zhang, Y., Wu, J., 2013. Numerical simulation in rockfall analysis: a close comparison of 2-D and 3-D DDA. Rock Mech. Rock. Eng. 46, 527–541. https://doi.org/10.1007/s00603-012-0360-9.
Collins, B.D., Sitar, N., 2007. Processes of coastal bluff erosion in weakly lithified sands, Pacifica, California, USA. Geomorphology 97 (3–4), 483–501, 10.1016/j.geomorph.2007.09.004.
Crosta, G.B., Agliardi, F., 2003. A methodology for physically based rockfall hazard assessment. Nat. Hazards Earth Syst. Sci. 3, 407–422. https://doi.org/10.5194/nhess-3-407-2003.
Crosta, G.B., Agliardi, F., 2004. Parametric evaluation of 3D dispersion of rockfall trajectories. Nat. Hazards Earth Syst. Sci. 4, 583–598. https://doi.org/10.5194/nhess-4-583-2004.
Crosta, G.B., Agliardi, F., Frattini, P., Lari, S., 2015. Key issues in rock fall modeling, Hazard and risk assessmnet for rockfall protection. Eng. Geol. Soc. Territory 2. https://doi.org/10.1007/978-3-319-09057-3_4.
Depountis, N., Nikolakopoulos, K., Kavoura, K., Sabatakakis, N., 2020. Description of a GIS-based rockfall hazard assessment methodology and its application in mountainous sites. Bull. Eng. Geol. Environ. 79, 645–658. https://doi.org/10.1007/s10064-019-01590-3.
Dorren, L.K.A., 2003. A review of rockfall mechanics and modelling approaches. Prog. Phys. Geogr. 27, 69–87. https://doi.org/10.1191/0309133303pp359ra.
Dorren, L.K.A., Domaa, U., Kronholm, K., Labiouse, V., 2013. Methods for predicting rockfall trajectories and run-out zones. In: Lambert, S., Nicot, F. (Eds.), Rockfall Engineering. ISTE Ltd. / John Wiley & Sons Inc, London, Hoboken, pp. 143–173. https://doi.org/10.1002/9781118601532.ch5.
Duperret, A., Genter, A., Martinez, A., Mortimore, R.N., 2004. Coastal chalk cliff instability in NW France: role of lithology, fracture pattern and rainfall. Geol. Soc. Lond. Eng. Geol. Spec. Publ. 20 (1), 33–55. https://doi.org/10.1144/GSL.ENG.2004.020.01.03.
Dussauge-Peisser, C., Grasso, C., Helmstetter, A., 2003. A statistical analysis of rockfall volume distributions: Implications for rockfall dynamics. J. Geophys. Res. Sol. EA. 108, 1–11. https://doi.org/10.1029/2001JB000650.
Emery, K.O., Kuhn, G.C., 1982. Sea cliffs: their processes, profiles, and classification. Geol. Soc. Am. Bull. 93, 644–654. https://doi.org/10.1130/0016-7606(1982)93<644:SCTPPA>2.0.CO;2.
Evans, S., Hungr, O., 1993. The assessment of rockfall hazard at the base of the talus slopes. Can. Geotech. J. 30, 620–636.
Ewalt Gray, J.M., O'Neill, K., Qiu, Z., 2017. Coastal residents' perceptions of the function of and relationship between engineered and natural infrastructure for coastal hazard mitigation. Ocean Coast. Manag. 146, 144–156. https://doi.org/10.1016/j.ocecoaman.2017.07.005.
Fanos, A.M., Pradhan, B., 2019. A novel rockfall hazard assessment using laser scanning data and 3D modelling in GIS. Catena 172, 435–450. https://doi.org/10.1016/j.catena.2018.09.012.
Feuillée, P., Rat, P., 1971. Structures et paléogéographies pyrénéo-cantabriques. In: Debyser, J., Le Pichon, X., Montardet, L. (Eds.), Histoire structural du Golfe de Gascogne, Tome 2. Publ. l'Inst. Français Pétrole, Coll. et Sémin., Technip, Paris, pp. 1–48.
Feurer, D., Vinatier, F., 2018. Joining multi-epoch archival aerial images in a single SfM block allows 3-D change detection with almost exclusively image information. ISPRS J. Photogramm. Remote Sens. 146, 495–506. https://doi.org/10.1016/j.isprsjprs.2018.10.016.
Fraternali, F., 2007. Free discontinuity finite element models in two-dimensions for in-plane crack problems. Theor. Appl. Fract. Mech. 47, 274–282. https://doi.org/10.1016/j.tafmec.2007.01.006.
Frattini, P., Crosta, G., Carrara, A., Agliardi, F., 2008. Assessment of rockfall susceptibility by integrating statistical and physically-based approaches. Geomorphology 94, 419–437. https://doi.org/10.1016/j.geomorph.2006.10.037.
Frattini, P., Crosta, G., Agliardi, F., 2012. Rockfall characterization and modeling. In: Clague, J.J., Stead, D. (Eds.), Landslides: Types, Mechanisms and Modeling. Cambridge University Press, Cambridge, pp. 267–281.
Galparsoro, I., Borja, A., Legorburu, I., Hernández, C., Chust, G., Liria, P., Uriarte, A., 2010. Morphological characteristics of the Basque continental shelf (Bay of Biscay, northern Spain); their implications for Integrated Coastal Zone Management. Geomorphology 118 (3–4), 314–329. https://doi.org/10.1016/j.geomorph.2010.01.012.
Garrido-Carretero, M.S., de Lacy-Pérez De Los Cobos, M.C., Borque-Arancón, M.J., Ruiz-Armenteros, A.M., Moreno-Guerrero, R., Gil-Cruz, A.J., 2019. Low-cost GNSS receiver in RTK positioning under the standard ISO-17123-8: A feasible option in geomatics. Measurement 137, 168–178. https://doi.org/10.1016/j.measurement.2019.01.045.
Genna, A., Capdeville, J.-P., Dubreuilh, J., Mallet, C., 2005. Évolution récente et actuelle de la côte basque française (analyse et perspectives). Compt. Rendus Geosci. 337, 1474–1483. https://doi.org/10.1016/j.crte.2005.08.010.
Glade, T., 2003. Vulnerability assessment in landslide risk analysis. Erde 134, 121–138.
González-Amuchastegui, M.J., Serrano-Cañadas, E., Edeso-Fito, J.M., Meaza-Rodriguez, G., 2005. Cambios en el nivel del mar durante el Cuaternario y morfología litoral en la costa oriental cantábrica (País Vasco y Cantabria). In: Sanjaume, E., Mateu, J.F. (Eds.), Geomorfologia Litoral i Quaternari, Libro Homenaje al Prof. V.M. Roselló i Verger. Publicaciones Universitat de València, Valencia, pp. 167–180.
Guo, Q., Wang, X., Zhang, H., Li, Z., Yang, S., 2009. Damage and conservation of the high cliff on the Northern area of Dunhuang Mogao Grottoes, China. Landslides 6, 89–100. https://doi.org/10.1007/s10346-009-0152-9.
Gutiérrez-Elorza, M., 2008. Geomorfología. Pearson/Prentice Hall, Madrid.
Guzzetti, F., Carrara, A., Cardinali, M., Reichenbach, P., 1999. Landslide hazard evaluation: a review of current techniques and their application in a multi-scale study, Central Italy. Geomorphology 31, 181–216. https://doi.org/10.1016/S0169-555X(99)00078-1.
Hampton, M.A., Griggs, G.B., 2004. Formation, evolution, and stability of coastal cliffs–status and trends. USGS Profess. Paper 1693, 1–4.
Henriques, M.H., dos Reis, R.P., Brilha, J., Mota, T., 2011. Geoconservation as an emerging geoscience. Geoheritage 3, 117–128. https://doi.org/10.1007/s12371-011-0039-8.
Hernández-Gutiérrez, L.E., Santamarta, J.C. (Eds.), 2015. Ingeniería geológica en terrenos volcánicos: Métodos, técnicas y experiencias en las Islas Canarias. Ilustre Colegio Oficial de Geólogos, Madrid.
Hoek, E., 1994. Strength of rock and rock masses. ISRM News J. 2 (2), 4–16.
Hungr, O., Evans, S., Hazzard, J., 1999. Magnitude and frequency of rockfalls and rock slides along the main transportation corridors of south-western British Columbia. Can. Geotech. J. 36, 224–238. https://doi.org/10.1139/t98-106.
ICOMOS, 2003. Principios para el análisis, conservación y restauración de las estructuras del patrimonio arquitectónico. Victoria Falls, Zimbabwe.
Jiang, Z., Du, J., Rieck, C., Bück, A., Tsotsas, E., 2020. PTV experiments and DEM simulations of the coefficient of restitution for irregular particles impacting on horizontal substrates. Powder Technol. 360, 352–365. https://doi.org/10.1016/j.powtec.2019.10.072.
Jing, R., Gong, Z., Zhao, W., Pu, R., Deng, L., 2017. Above-bottom biomass retrieval of aquatic plants with regression models and SfM data acquired by a UAV platform – A case study in Wild Duck Lake Wetland, Beijing, China. ISPRS J. Photogramm. Remote Sens. 134, 122–134. https://doi.org/10.1016/j.isprsjprs.2017.11.002.
Kaur, H., Gupta, S., Parkash, S., Thapa, 2018. Application of geospatial technologies for multi-hazard mapping and characterization of associated risk at local scale. Ann. GIS 24 (1), 33–46. https://doi.org/10.1080/19475683.2018.1424739.
Keskin, I., 2013. Evaluation of rockfalls in an urban area: the case of Boğaziçi (Erzincan/Turkey). Environ. Earth Sci. 70, 1619–1628. https://doi.org/10.1007/s12665-013-2247-9.
Kim, K., Choi, J., Chung, J., Koo, G., Bae, I.-H., Sohn, H., 2018. Structural displacement estimation through multi-rate fusion of accelerometer and RTK-GPS displacement and velocity measurements. Measurement 130, 223–235. https://doi.org/10.1016/j.measurement.2018.07.090.
Kirchner, K., Kubalíková, L., 2013. Relief assessment methodology with respect to geoheritage based on example of the Deblínská vrchovina highland. In: Fialová, J., Kubíčková, H. (Eds.), Public Recreation and Landscape Protection – with Man Hand in Hand Conference Proceeding. Brno, pp. 131–141.
Kirchner, K., Kubalíková, L., 2015. Geomythology: A useful tool for geoconservation and geotourism purposes. In: Fialová, J., Pernicová, D. (Eds.), Public Recreation and Landscape Protection – with Man Hand in Hand. Conference Proceeding, Brno, pp. 68–74.
Kobayashi, Y., Harp, E., Kagawa, T., 1990. Simulation of Rockfalls triggered by earthquakes. Rock. Mech. Rock. Eng. Int. 19, 313–320. https://doi.org/10.1007/BF01020418.
Kong, D., Wu, F., Saroglou, C., 2020. Automatic identification and characterization of discontinuities in rock masses from 3D point clouds. Eng. Geol. 265, 105442. https://doi.org/10.1016/j.enggeo.2019.105442.
Kubalíková, L., 2013. Geomorphosite assessment for geotourism purposes. Czech J. Tour. 2, 80–104. https://doi.org/10.2478/cjot-2013-0005.
Lambert, S., Bourrier, F., 2013. Design of rockfall protection embankments: A review. Eng. Geol. 154, 77–88. https://doi.org/10.1016/j.enggeo.2012.12.012.

Lan, H., Martin, C.D., Lim, C.H., 2007. RockFall analyst: A GIS extension for three-dimensional and spatially distributed rockfall hazard modeling. Comput. Geosci. 33, 262–279. https://doi.org/10.1016/j.cageo.2006.05.013.
Li, L., Lan, H., 2015. Probabilistic modeling of rockfall trajectories: a review. Bull. Eng. Geol. Environ. 74, 1163–1176. https://doi.org/10.1007/s10064-015-0718-9.
Li, X., Dong, M., Jiang, D., Li, S., Shang, Y., 2020. The effect of surface roughness on normal restitution coefficient, adhesion force and friction coefficient of the particle-wall collision. Powder Technol. 362, 17–25. https://doi.org/10.1016/j.powtec.2019.11.120.
Lorentz, J., Plassiard, J.-P., Muquet, L., 2010. An innovative design process for rockfall embankments: application in the protection of a building at Val d'Isère. In: Proceedings of the 3rd Euro Mediterranean Symposium on Advances in Geomaterial sand Structures—AGS, Djerba, Tunisia, pp. 277–282.
Luckman, B.H., 2013. Processes, Transport, Deposition and Landforms: Rockfall. Treatise Geomorphol. 7, 174–182. https://doi.org/10.1016/B978-0-12-374739-6.00162-7.
Margottini, C., Vilímek, V., 2014. The ICL Network on "Landslides and Cultural & Natural Heritage" (LACUNHEN). Lanslides 11, 933–938. https://doi.org/10.1007/s10346-014-0510-0.
Margottini, C., Gigli, G., Ruther, H., Spizzichino, D., 2016. Advances in sustainable conservation practices in rupestrian settlements inscribed in the UNESCO's World Heritage List. Procedia Earth Planet. Sci. 16, 52–60. https://doi.org/10.1016/j.proeps.2016.10.006.
Masuya, H., Amanuma, K., Ishikawa, Y., Tsuji, T., 2009. Basic rockfall simulation with consideration of vegetation and application to protection measure. Nat. Hazards Earth Syst. Sci. 9, 1835–1843. https://doi.org/10.5194/nhess-9-1835-2009.
Michoud, C., Derron, M.H., Horton, P., Jaboyedoff, M., Baillifard, F.J., Loye, A., Nicolet, P., Pedrazzini, A., Queyrel, A., 2012. Rockfall hazard and risk assessments along roads at a regional scale: example in Swiss Alps. Nat. Hazards Earth Syst. Sci. 12, 615–629. https://doi.org/10.5194/nhess-12-615-2012.
Morales, T., Uribe-Etxebarria, G., Uriarte, J.A., Fernández de Valderrama, I., 2004. Geomechanical characterisation of rock masses in Alpine regions: the Basque Arc (Basque-Cantabrian basin, Northern Spain). Eng. Geol. 71, 343–362. https://doi.org/10.1016/S0013-7952(03)00160-1.
Morales, T., Uriarte, J.A., Damas, L., Antigüedad, I., 2018. Taludes inestables y patrimonio cultural: cómo y hasta dónde actuar. Una visión desde las Galerías Punta Begoña (Getxo, Bizkaia). In: Proc. of the VI Congreso del GEIIC, Vitoria-Gasteiz, pp. 426–433.
Orue-Etxebarria, X., Alegret, L., Apellaniz, E., Arenillas, I., Baceta, J.I., Bernaola, G., Caballero, F., Dinarès-Turell, J., Martín-Rubio, M., Molina, E., Ortíz, S., Pujalte, V., Schmitz, B., 2007. The Zumaia Section: a robust candidate for the placement of the Danian/Selandian and Selandian/Thanetian boundaries. International Workshop of the Paleocene Working Group, Zumaia, pp. 33–35. Volume of Abstracts.
Panizza, M., 2001. Geomorphosites: Concepts, methods and example of geomorphological survey. Chin. Sci. Bull. 46, 4–5. https://doi.org/10.1007/BF03187227.
Pedoja, K., Husson, L., Johnson, M.E., Melnick, D., Witt, C., Pochat, S., Nexer, M., Delcaillau, B., Pinegina, T., Poprawski, Y., Authemayou, C., Elliot, M., Regard, V., Garestier, F., 2014. Coastal staircase sequences reflecting sea-level oscillations and tectonic uplift during the Quaternary and Neogene. Earth-Sci. Rev. 132, 13–38. https://doi.org/10.1016/j.earscirev.2014.01.007.
Pfeiffer, T.J., Bowen, T.D., 1989. Computer simulation of rockfalls. Bull. Assoc. Eng. Geol. 26, 135–146.
Pham, B.T., Pradhan, B., Tien Bui, D., Prakash, I., Dholakia, M.B., 2016. A comparative study of different machine learning methods for landslide susceptibility assessment: a case study of Uttarakhand area (India). Environ. Model. Softw. 84, 240–250. https://doi.org/10.1016/j.envsoft.2016.07.005.
Pierre, G., Lahousse, P., 2006. The role of groundwater in cliff instability: an example at Cape Blanc-Nez (Pas-de-Calais, France). Earth Surf. Proc. Landforms J. Br. Geomorphol. Res. Group 31 (1), 31–45. https://doi.org/10.1002/esp.1229.
Porter, N.J., Trenhaile, A.S., 2007. Short-term rock surface expansion and contraction in the intertidal zone. Earth Surface Processes and Landforms: the Journal of the British Geomorphological Research. Group 32 (9), 1379–1397. https://doi.org/10.1002/esp.1479.
Pujalte, V., Baceta, J.I., Dinarès-Turell, J., Orue-Etxebarria, X., Parés, J.M., Payros, A., 1995. Biostratigraphic and magnetostratigraphic intercalibration of latest Cretaceous and Paleocene depositional sequences from the deep-water Basque basin, western Pyrenees. Spain. Earth Planet. Sci. Lett. 136, 17–30.
Ramírez del Pozo, J., 1973. Síntesis geológica de la provincia de Álava. Obra cultural de la Caja de ahorros de la Ciudad de Vitoria, Vitoria-Gasteiz.
Raquet, J., Lachapelle, G., 2001. RTK positioning with multiple reference stations. GPS World 12, 48–53.
Rebouças, G.F.S., Santos, I.F., Thomsen, J.J., 2019. Unilateral vibro-impact systems – Experimental observations against theoretical predictions based on the coefficient of restitution. J. Sound Vib. 440, 346–371. https://doi.org/10.1016/j.jsv.2018.10.037.
REDMAR, 2005. Resumen de parámetros relacionados con el nivel del amr y la marea que afectan a las condiciones de diseño y explotación portuaria. Puertos del Estado 19. https://www.puertos.es.
Reichenbach, P., Rossi, M., Malamud, B.D., Mihir, M., Guzzetti, F., 2018. A review of statistically-based landslide susceptibility models. Earth Sci. Rev. 180, 60–91. https://doi.org/10.1016/j.earscirev.2018.03.001.
RocPro3D, 2014. RocPro3D software. http://www.rocpro3d.com/rocpro3d_en.php.
RocScience, 2004. RocFall software for risk analysis of falling rock on steep slope. In: RocScience's User's Guide. https://www.rocscience.com/software/rocfall.
RocScience, 2013. Dips, Analyze orientation-based geological data. In: RocScience's User's Guide. https://www.rocscience.com/software/dips.
Rosser, N.J., Petley, D.N., Lim, M., Dunning, S.A., Allison, R.J., 2005. Terrestrial laser scanning for monitoring the process of hard rock coastal cliff erosion. Q. J. Eng. Geol. Hidrogeol. 38, 363–375. https://doi.org/10.1144/1470-9236/05-008.
Schmitz, B., Molina, E., Von Salis, K., 1998. The Zumaya section in Spain: a possible global stratotype section for the Selandian and Thanetian stages. Newsl. Stratigr. 36, 35–42. https://doi.org/10.1127/nos/36/1998/35.
Schmitz, B., Pujalte, V., Molina, E., Monechi, S., Orue-Etxebarria, X., Speijer, R.P., Alegret, L., Apellaniz, E., Arenillas, I., Aubry, M.-P., Baceta, J.I., Berggren, W.A., Bernaola, G., Caballero, F., Clemmensen, A., Dinarès-Turell, J., Dupuis, Ch., Heilmann-Clausen, C., Hilario-Orús, A., Knox, R., Martín-Rubio, M., Ortiz, S., Payros, A., Petrizzo, M.R., Von Salis, K., Sprong, J., Steurbaut, E., Thomsen, E., 2011. The Global Stratotype Sections and Points for the bases of the Selandian (Middle Paleocene) and Thanetian (Upper Paleocene) stages at Zumaia, Spain. Episodes 34, 220–243. https://doi.org/10.18814/epiiugs/2011/v34i4/002.
Shirzadi, A., Saro, L., Hyun Joo, O., Chapi, K., 2012. A GIS-based logistic regression model in rock-fall susceptibility mapping along a mountainous road: Salavat Abad case study, Kurdistan, Iran. Nat. Hazards 64, 1639–1656. https://doi.org/10.1007/s11069-012-0321-3.
Spadari, M., Kardani, M., De Carteret, R., Giacomini, A., Buzzi, O., Fityus, S., Sloan, S.W., 2013. Statistical evaluation of rockfall energy ranges for different geological setting of New South Wales. Austr. Eng. Geol. 158, 57–65. https://doi.org/10.1016/j.enggeo.2013.03.007.
Stoffel, M., Schneuwly, D.M., Bollschweiler, M., 2010. Assessing rockfall activity in mountain forest – implications for hazard assessment. In: Stoffel, M., Bollschweiler, M., Butler, D.R., Luckman, B. (Eds.), Tree Rings and Natural Hazards: A state of the art (Advances in Global Change Research Book 41). Springer, Dordrecht, pp. 139–155. https://doi.org/10.1007/978-90-481-8736-2_13.
Sunamura, T., 1992. Geomorphology of Rocky Coasts. John Wiley and Sons, New York, NY.
Sunamura, T., 2015. Rocky coast processes: with special reference to the recession of soft rock cliffs. Proc. Japan Acad. Ser. B Phys. Biol. Sci. https://doi.org/10.2183/pjab.91.481.
Tomás, R., Riquelme, A., Cano, M., Abellán, A., Jordá, L., 2016. Structure from Motion (SfM): una técnica fotogramétrica de bajo coste para la caracterización y monitoreo de macizos rocosos. In: 10° Simposio Nacional Ingeniería Geotécnica. A Coruña, pp. 209–216.
Touili, N., Baztan, J., Vanderlinden, J.-P., Kane, I.O., Diaz-Simal, P., Pietrantoni, L., 2014. Public perception of engineering-based coastal flooding and erosion risk mitigation options: Lessons from three European coastal settings. Coast. Eng. 87, 205–209. https://doi.org/10.1016/j.coastaleng.2014.01.004.
Trenhaile, A.S., 2010. The effect of Holocene changes in relative sea level on the morphology of rocky coasts. Geomorphology 114 (1–2), 30–41. https://doi.org/10.1016/j.geomorph. 2009.02.003.
Valente, D.S.M., Momin, A., Grift, T., Hansen, A., 2020. Accuracy and precision evaluation of two low-cost RTK global navigation satellite systems. Comput. Electron. Agric. 168, 105142. https://doi.org/10.1016/j.compag.2019.105142.
Varnes, D.J., 1978. Slope movement types and processes. In: Schuster, R.L., Krizek, R.J. (Eds.), Landslides. Analysis and control: National Research Council, 176. Transportation Research Board, Special Report, Washington, D.C., pp. 11–33. http://onlinepubs.trb.org/Onlinepubs/sr/sr176/176-002.pdf
Volkwein, A., Schellenbger, K., Labiouse, V., Agliardi, F., Berger, F., Bourrier, F., Dorren, L.K.A., Jaboyedoff, M., 2011. Rockfall characterisation and structural protection- a review. Nat. Hazards Earth Syst. Sci. 11, 2617–2651. https://doi.org/10.5194/nhess-11-2617-2011.
Volkwein, A., Gerber, W., Klette, J., Spescha, G., 2019. Review of Approval of Flexible Rockfall Protection Systems According to ETAG 027. Geosciences 9, 49. https://doi.org/10.3390/geosciences9010049.
Wang, L., Zheng, Z., Yu, Y., Liu, T., Zhang, Z., 2020. Determination of the energetic coefficient of restitution of maize grain based on laboratory experiments and DEM simulations. Powder Technol. 362, 645–658. https://doi.org/10.1016/j.powtec.2019.12.024.
Westoby, M.J., Brasington, J., Glasser, N.F., Hambrey, M.J., Reynolds, J.M., 2012. 'Structure-from-Motion' photogrammetry: A low-cost, effective tool for geoscience applications. Geomorphology 179, 300–314. https://doi.org/10.1016/j.geomorph.2012.08.021.
Wimbledon, W.A.P., Smith-Meyer, S., 2012. Geoheritage in Europe and its conservation. ProGEO, Oslo.
Wu, M., Liu, W., Wu, R., Zhang, X., 2019. Tightly combined GPS/Galileo RTK for short and long baselines: Model and performance analysis. Adv. Space Res. 63, 2003–2020. https://doi.org/10.1016/j.asr.2018.12.008.
Young, A.P., 2018. Decadal-scale coastal cliff retreat in southern and central California. Geomorphology 300, 164–175. https://doi.org/10.1016/j.geomorph.2017.10.010.
Young, A.P., Guza, R.T., O'Reilly, W.C., Flick, R.E., Gutierrez, R., 2011. Short-term retreat statistics of a slowly eroding coastal cliff. Nat. Hazards Earth Syst. Sci. 11 (1), 205–217. https://nhess.copernicus.org/articles/11/205/2011/.
Zhang, P., Du, K., Tannant, D.D., Zhu, H., Zheng, W., 2018. Automated method for extracting and analysing the rock discontinuities from point clouds based on digital surface model of rock mass. Eng. Geol. 239, 109–118. https://doi.org/10.1016/j.enggeo.2018.03.020.
Zhang, Z., Luo, J., Chen, B., 2020. Spatially explicit quantification of total soil erosion by RTK GPS in win and water eroded croplands. Sci. Total Environ. 702, 134716. https://doi.org/10.1016/j.scitotenv.2019.134716.